Search for the decay $\pi^0 \to e^+e^-$

Carsten Niebuhr, Ralph Eichler, Larry Felawka,* Tadeusz Kozlowski,†
Stephen Playfer, and H. Kristian Walter
Institut für Mittelenergiephysik der Eidgenössischen Technischen Hochschule Zürich, CH-5232 Villigen PSI, Switzerland

Andries van der Schaaf, Stephan Egli, Martin Grossmann-Handschin, Erwin Hermes,
Franz Muheim, Henk Pruys, and Detlef Vermeulen
Physik-Institut der Universität Zürich, CH-8001 Zürich, Switzerland

Wilhelm Bertl and Nicolas Lordong
Paul Scherrer Institut, CH-5232 Villigen PSI, Switzerland

Jacques Martino
Centre d'Études Nucléaires Saclay, Département de Physique Nucléaire et de Hautes Énergies, F-91191 Gif-sur-Yvette, France

Reena Meijer Drees and Chris Waltham
Physics Department, University of British Columbia, Vancouver, British Columbia, Canada V6T 2A6

Ulrich Bellgardt
III. Physikalisches Institut B der Rheinisch-Westfälischen Technischen Hochschule Aachen, D-5100 Aachen, West Germany
(SINDRUM Collaboration)
(Received 13 April 1989)

The reaction $\pi^- p \to \pi^0 n$ at rest was used as a source of tagged monoenergetic π^0's in a search for the decay $\pi^0 \to e^+e^-$ with the SINDRUM I spectrometer. The measurement resulted in $B_{\pi^0 \to e^+e^-} \equiv \Gamma_{\pi^0 \to e^+e^-}/\Gamma_{\pi^0 \to 2\gamma} < 1.3 \times 10^{-7}$ (90% confidence level), consistent with the QED prediction $B_{\pi^0 \to e^+e^-} = (6.5 \pm 0.5) \times 10^{-8}$. The combined result of two previous measurements, $B_{\pi^0 \to e^+e^-} = (1.8^{+0.7}_{-0.6}) \times 10^{-7}$, had suggested sizable additional contributions to the decay amplitude. This possibility now seems unlikely.

I. INTRODUCTION

The decay of pseudoscalar mesons into lepton pairs $P^0 \to l^+l^-$ is thought to proceed dominantly as a higher-order electromagnetic process via a 2γ intermediate state. For on-shell photons quantum electrodynamics gives a value for $\Gamma_{P^0 \to l^+l^-}/\Gamma_{P^0 \to 2\gamma}$, the branching ratio relative to the two-photon decay mode, from unitarity only: $B_{\text{unit}} = \{\alpha r \ln[(1+\beta)/(1-\beta)]\}^2/2\beta$, where r is the ratio between the lepton and meson masses and $\beta = \sqrt{1-4r^2}$ is the lepton velocity in the meson c.m. system. The contribution from off-shell photons increases the predicted value of the branching ratio by about 30% (see Ref. 1 for a review). For the decay $\pi^0 \to e^+e^-$, for which $B_{\text{unit}} = 4.75 \times 10^{-8}$, a large number of calculations have been made using vector-meson dominance,[2] dispersion relations,[3] and asymptotic QCD arguments.[2,4] Despite this wide range of approaches the results for the branching ratio only vary between 6.2×10^{-8} (Ref. 4) and 6.9×10^{-8} (Ref. 3). The insensitivity of the decay amplitude to details of the model is discussed in Ref. 5.

The large helicity suppression of the electromagnetic amplitude of the decay $\pi^0 \to e^+e^-$ has led to speculations that additional contributions might be important. The effect of most other couplings is small, i.e., weak neutral currents ($B_{\pi^0 \to e^+e^-} \sim 10^{-15}$) (Ref. 4) or axion couplings ($B_{\pi^0 \to e^+e^-} \leq 5 \times 10^{-11}$) (Refs. 4 and 6). However, anomalous quark-lepton couplings could lead to significant enhancements of the value for the branching ratio.[7-10] Bergström has shown that a sizable contribution could only come from a new pseudoscalar interaction.[4] A branching ratio below the unitarity value would be a sign of *CP*-violating neutral currents.[11,7]

Because of the small branching ratios only three decay modes $P^0 \to l^+l^-$ have been observed so far. Table I shows the experimental results.[12] A discrepancy could exist in the case of the decay $\pi^0 \to e^+e^-$ where the measured branching ratio is roughly three times larger than the QED prediction, but with a large error. Fischer *et al.*[13] at CERN used tagged π^0's from $K^+ \to \pi^+\pi^0$ decays in flight and quote a value of $B_{\pi^0 \to e^+e^-} = (2.23^{+2.4}_{-1.1}) \times 10^{-7}$ (90% confidence level) from a signal of six events. Frank *et al.*[14] at LAMPF produced π^0's by $\pi^- p \to \pi^0 n$ in flight and obtain $B_{\pi^0 \to e^+e^-} = (1.7 \pm 0.6 \pm 0.3) \times 10^{-7}$ on the basis of 59 ± 21 events on a large background. A third experiment,[15] done with the OMICRON spectrometer at CERN, also studied $\pi^- p \to \pi^0 n$ in flight and quotes an upper limit of

TABLE. I. Experimental values for the branching ratio of the decay of pseudoscalar mesons into lepton pairs relative to the 2γ width (Ref. 12). Processes for which only upper limits exist have been left out.

Decay	$\left[\frac{\Gamma_{P^0\to l^+l^-}}{\Gamma_{P^0\to 2\gamma}}\right]_{\text{expt}}$	B_{unit}	Ratio
$\pi^0 \to e^+e^-$	$(1.8\pm^{0.7}_{0.6})\times 10^{-7}$	4.75×10^{-8}	$3.8\pm^{1.5}_{1.3}$
$\eta \to \mu^+\mu^-$	$(1.7\pm 0.5)\times 10^{-5}$	1.11×10^{-5}	$1.5\pm^{0.5}_{0.4}$
$K_l^0 \to \mu^+\mu^-$	$(1.7\pm^{0.4}_{0.3})\times 10^{-5}$	1.20×10^{-5}	$1.4\pm^{0.4}_{0.3}$

$B_{\pi^0\to e^+e^-} < 5.3\times 10^{-7}$ (90% confidence level). The combined result of the first two measurements, $B_{\pi^0\to e^+e^-} = (1.8\pm^{0.7}_{0.6})\times 10^{-7}$, indicates that nonelectromagnetic contributions might be involved. To reach definite conclusions on such contributions the large experimental uncertainty has to be reduced.

A new $\pi^0 \to e^+e^-$ experiment has been performed with the SINDRUM I spectrometer at the Paul Scherrer Institut (PSI) (Ref. 16). The π^0 production process in this experiment is $\pi^- p \to \pi^0 n$ at rest; so no analysis of the incoming beam is required. The π^0's have a yield per π^- of 60.7% and are tagged by detection of the 418-keV neutron emitted in the opposite direction. The major disadvantage is the enormous background from the reaction $\pi^- p \to e^+e^- n$ which has an e^+e^- mass distribution with a rate at the π^0 mass of 2.6×10^{-6} per MeV/c^2 and per π^0 produced. By measuring the neutron with a time-of-flight resolution of 1.3% [full width at half maximum (FWHM)] indirectly an e^+e^- mass resolution of 90 keV/c^2 (FWHM) is obtained; this gives a continuum background level of 2.3×10^{-7}. Unfortunately, the price for the neutron detection in our experiment is a reduction in acceptance by 4 orders of magnitude. The e^+e^- opening-angle distribution has a pronounced peak at its minimum value of $2\arccos\beta_{\pi^0}$. The low value of $\beta_{\pi^0}=0.204$ for the reaction $\pi^- p \to \pi^0 n$ at rest results in a large value for the minimum e^+e^- opening angle of 156.5°. This condition simplifies the trigger for data readout and is favorable for the resolution of the direct e^+e^- mass determination, which helps to discriminate against background from other π^0 decay modes. Since the momenta of all three particles in the final state are measured there are three additional constraints, e.g., coplanarity, which further suppress the π^0 background. Monte Carlo simulation shows that most of the remaining π^0 background involves external γ conversions in liquid hydrogen. The rate of these events has been reduced to a negligible level by minimizing the target dimensions and improving on vertex resolution.

The main background process $\pi^- p \to e^+e^- n$ gives a precise normalization since the acceptances of the detection system for $\pi^- p \to e^+e^- n$ and $\pi^- p \to \pi^0 n$ followed by $\pi^0 \to e^+e^-$ are nearly identical. In addition the resolution functions can be obtained from $\pi^- p \to e^+e^- n$ events with neutron momenta around the π^0 resonance. As a consequence no Monte Carlo simulation is required to determine the response functions of the detection system or the sensitivity of the measurement.

II. DETECTION SYSTEM AND ON-LINE EVENT SELECTION

The experimental setup is shown in Fig. 1. The π^0's are produced by charge exchange, $\pi^- p \to \pi^0 n$, using a beam of negative pions stopped in liquid hydrogen. The target cell has the shape of a 12-cm-long cylinder with a radius of 19 mm concentric with the beam axis and closed by a half sphere at the side of the beam entrance. The center of this half sphere is located 10 cm upstream of the center of the SINDRUM I spectrometer to optimize the acceptance for decays of π^0's moving downstream. Since the major background from π^0 decays comes from γ conversion in liquid hydrogen (Compton effect and pair production), the value of the target radius was chosen as a compromise between the stop rate and the level of this external background. The 95-MeV/c π^- beam passed through a 5-mm-thick lead moderator giving the highest stop density at the beginning of the target. This way the loss of neutrons scattered from hydrogen was minimized (418-keV neutrons have an attenuation length of 6.1 cm in lead and 3.4 cm in liquid hydrogen). About 10% of the incident 5×10^6 π^- s^{-1} stopped in the first 5 cm of the target.

The SINDRUM I detector was originally designed for a search for the decay $\mu \to 3e$ and has been described in detail in Ref. 17. For this experiment the two innermost cylindrical wire chambers were replaced by chambers with smaller radii and wire spacing giving improvements in vertex and momentum resolutions. The first one has a wire spacing of 1 mm and a radius of 37.3 mm, which leads to a lower threshold for the detection of hits from additional charged particles between 2 and 6 MeV/c, depending on vertex position and emission angle. Three of the five wire chambers give full three-dimensional information for every hit using cathode strip readout. The momentum resolution was further improved by increas-

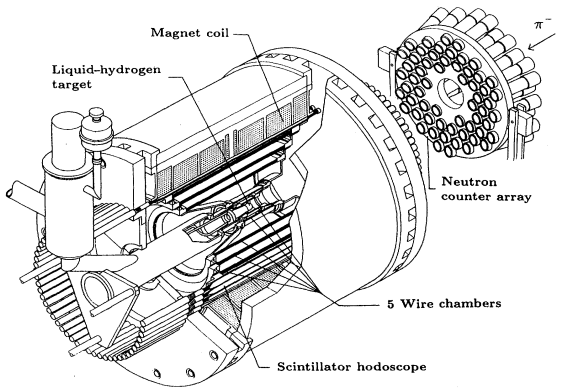

FIG. 1. The SINDRUM I spectrometer with neutron detector.

ing the magnetic field from a value of 3.3 to 6.8 kG. The geometrical acceptance of the spectrometer for $\pi^0 \to e^+e^-$ decays depends on direction and position of the decaying π^0. For decays tagged by the neutron detector the acceptance in the first 3 cm of the target is 70% as defined by the solid angle of the hodoscope. In the following 2.5 cm the acceptance drops linearly to zero due to the finite length of the innermost wire chamber.

The neutron detector was an array of 60 plastic-scintillator disks grouped around the beam pipe in front of the last beam quadrupole at a distance of 132 cm from the target. The light produced by a recoil proton with energy below 418 keV is equal to the light output for an electron of 50 keV or less.[18] In order to obtain the required detection efficiency and time resolution an extremely high light collection efficiency is necessary. In addition the uncertainty in the neutron flight path due to the detector thickness should be minimized. For these reasons the Pilot U (Ref. 19) scintillators were 6.5-mm-thick disks with a diameter of 44 mm positioned directly in front of the cathodes of 2-in. photomultipliers. This way a yield of two photoelectrons per keV electron energy was obtained.[20] The resulting total neutron solid angle was 4.2×10^{-3} of 4π sr. The timing discriminators which were especially designed for the experiment incorporate three levels of amplitude discrimination: the lowest one defining the time signal and the others defining an amplitude window corresponding to 100–600-keV recoil-proton energy. In this window the count rate is dominated by photon interactions, so veto counters against charged particles were not necessary. The efficiency for neutron detection drops smoothly in the range of kinetic energies selected by the time-of-flight window, from 15% at 400 keV to 12% at 800 keV.

The trigger for data readout required the occurrence of a neutron signal in a time interval between 80 and 170 ns after the detection of a lepton pair with an opening angle in the $r\phi$ plane perpendicular to the beam axis of at least 135°. Neutrons from the reaction $\pi^-p \to \pi^0 n$ have a time of flight of about 148 ns. Since the neutrons are detected at angles θ relative to the beam direction larger than 165.5° the e^+e^- pairs from $\pi^0 \to e^+e^-$ have opening angles of at least 174.1° in the $r\phi$ plane. A programmable FASTBUS track preselector was used to search for track candidates in the pattern of the hodoscope strips and groups of 8 or 16 anode wires. For each track the angle of emission was stored. The opening-angle requirement was then tested by a general purpose FASTBUS processor with a mean decision time of 50 μs. Before going to tape the data were filtered by a full analysis of the information in the $r\phi$ projection. The filter program required two tracks with a time difference within 1.6 ns and an $r\phi$ opening angle larger than 165°. The final event rate was about 0.1 s^{-1}. In total about 4×10^8 tagged π^0's were registered during the measuring period of 50 days.

III. OFF-LINE EVENT SELECTION

In the off-line analysis the particle trajectories in the spectrometer were reconstructed in all three dimensions using the coordinates along the detector axis deduced from the amplitudes on the cathode strips. Thanks to the relatively simple topologies in this experiment the reconstruction efficiency was as high as 97%. The neutron velocity has been determined using the measured position of the e^+e^- vertex in the calculation of the flight path after correction of the time of flight for the walk in the neutron time signal. Using the fitted track parameters events were selected containing e^+e^- combinations with a minimum opening angle of 140°, a maximum time difference of 1.25 ns, and a distance of closest approach (DCA) to a common vertex inside the hydrogen target of less than 1.1 mm. These cuts correspond to 3–5 standard deviations for $\pi^0 \to e^+e^-$ events.

The remaining event sample was analyzed in two steps. First events of the reaction $\pi^-p \to e^+e^-n$ were selected which contain $\pi^-p \to \pi^0 n$, followed by $\pi^0 \to e^+e^-$ as well. The distribution of β_n was then analyzed assuming contributions from $\pi^-p \to e^+e^-n$ and π^0 decays. The π^0 decays contain the decay $\pi^0 \to e^+e^-$ and a series of other π^0 decay modes for which the additional particles have such a low energy that they remained unnoticed. Under the assumption of a three-body (e^+e^-n) final state the total kinetic energy $T_{\rm tot}$ has been calculated using the e^+e^- pair only. For final states with additional photons or electrons this calculation results in a value which is always less than the available kinetic energy of 137.3 MeV. The $T_{\rm tot}$ spectrum (see Fig. 2) shows an enhancement of $\approx$6400 three-body events at the kinematical end point. These events are due to the reaction $\pi^-p \to e^+e^-n$ with a possible contribution from the decay $\pi^0 \to e^+e^-$. The continuum has contributions from various π^0 decays: $\pi^0 \to e^+e^-\gamma$, $\pi^0 \to e^+e^-e^+e^-$, and decays involving external γ conversions (for example, $\pi^0 \to e^+e^-\gamma$ followed by Compton scattering in the target). Events with more than five hits in the innermost wire chamber were rejected since they are dominated by π^0 decays with additional low-momentum tracks. Because of the high level of random hits in this detector the multiplicity requirement removes about 2% of the e^+e^-n events. This loss would rise to about 50% if events with more than two

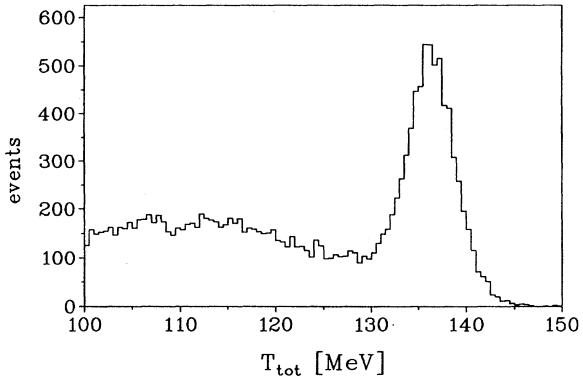

FIG. 2. Distribution of the total kinetic energy $T_{\rm tot}$ determined from the e^+e^- measurement only.

hits would be rejected.

The distributions of the remaining observables, used to remove background events from π^0 decays and e^+e^-n events with accidental or scattered neutrons, are shown in Fig. 3. For these histograms events were selected with $T_{\rm tot} > 125$ MeV and β_n in two regions around the π^0 peak: $0.0265 < \beta_n < 0.0295$ or $0.0304 < \beta_n < 0.0415$. For e^+e^-n events the neutron is emitted with a momentum of $-(\mathbf{p}_{e^+}+\mathbf{p}_{e^-})$. The error in the neutron direction is decomposed into the component $\theta_\parallel$ in the e^+e^- plane [Fig. 3(a)] and the component $\theta_\perp$ perpendicular to it [Fig. 3(b)]. Both distributions show Gaussian peaks of direct neutrons on top of a constant background of scattered and accidental neutrons. The resolution of $\theta_\perp$ ($\sigma = 3.2°$) is dominated by the e^+e^- angular resolution in the $r\phi$ plane ($\sigma = 0.8°$) whereas the resolution of $\theta_\parallel$ ($\sigma = 3.6°$) is mainly determined by the momentum resolution in the $r\phi$ plane ($\sigma_p/p \simeq 2\%$). The contribution from the error in the neutron measurement is only 0.5° in both projections. The remaining observable, the neutron velocity, was tested using the information of the three angles of emission, as follows. The velocity of the state decaying into the e^+e^- pair, $\beta_{e^+e^-}$, can be determined both from the neutron velocity

$$\beta^{\rm TOF}_{e^+e^-} = \frac{\beta_n}{E_{\pi^-p}/(\gamma_n m_n) - 1} \tag{1}$$

and from the emission angles

$$\beta^{\theta}_{e^+e^-} = \frac{\cos\frac{\theta^+ + \theta^-}{2}}{\cos\frac{\theta^+ - \theta^-}{2}} , \tag{2}$$

where $E_{\pi^-p} = 1077.8$ MeV is the total energy of the π^-p atom and $\theta^\pm$ is the angle between $e^\pm$ and the neutron. The distribution of the difference between these two values for $\beta_{e^+e^-}$ is shown in Fig. 3(c). Three contributions can be distinguished: a peak of events with unperturbed neutrons, a flat contribution from accidental neutrons, and a contribution with $\beta^{\rm TOF}_{e^+e^-} < \beta^{\theta}_{e^+e^-}$ from scattered neutrons. The width of the peak ($\sigma = 1.3\%$) is dominated by the resolution of $\beta^{\theta}_{e^+e^-}$ which is determined by the z resolution of the wire chambers.

Only events with a probability for the neutron to be unperturbed which is larger than 50% have been accepted. For this purpose a modified χ^2 expression was used, which accounts for the nonuniform $\beta^{\theta}_{e^+e^-} - \beta^{\rm TOF}_{e^+e^-}$ distribution of the scattered neutrons:

$$\chi^2(x_1,x_2,x_3) = \ln \prod_{i=1}^{3} R_i(x_i) = \sum_{i=1}^{3} \ln R_i(x_i) , \tag{3}$$

where

$$\begin{aligned} &x_1 = \theta_\parallel, \quad x_2 = \theta_\perp, \quad x_3 = \beta^{\theta}_{e^+e^-} - \beta^{\rm TOF}_{e^+e^-} , \\ &R_i(x_i) \propto \frac{B_i(x_i)}{S_i(x_i)}, \quad S_i(x_i) \propto e^{-x_i^2/(2\sigma_i^2)} , \\ &B_{1,2}(x_{1,2}) = \text{const} , \\ &B_3(x_3) \propto 1 + k\int_{-\infty}^{x_3} e^{-x^2/(2\sigma_3^2)} dx . \end{aligned} \tag{4}$$

The functions $S_i(x_i)$ and $B_i(x_i)$ are the x_i distributions for unperturbed and background neutrons, respectively. The value for the parameter k, which determines the relative yield of scattered and accidental neutrons, has been adapted to the measured x_3 distribution. The ratios $R_i(x_i)$ have been normalized by the condition $\min[R(x)] = 1$, so the first two terms of χ^2 are simply $(x_{1,2}/\sigma_{1,2})^2/2$. The functions B_i, $S_i + B_i$, and R_i are shown in Fig. 3. In the variable $(\chi^2)^{3/2}$ [see Fig. 3(d)] events with unperturbed neutrons peak at zero whereas events with accidental or scattered neutrons should have a flat distribution. The signal-to-background ratio reaches the value 1 for $\chi^3 \simeq 35$.

For three-body events with unperturbed neutrons ($\chi^3 \leq 35$) the total kinetic energy $T_{\rm tot}$ has been calculated with improved resolution using a constrained fit of the three momenta. Since the remaining background from π^0 decays is dominated by events with external photon conversions, which have a broadened DCA distribution, the π^0 background has been minimized using both $T_{\rm tot}$ and DCA as shown by the contour in Fig. 4. The contour follows a line of constant signal-to-background ratio in the approximation of Gaussian $T_{\rm tot}$ and DCA distributions for the signal, and a background distribution which is constant for $T_{\rm tot} \leq 137.3$ MeV and Gaussian for $T_{\rm tot} \geq 137.3$ MeV.

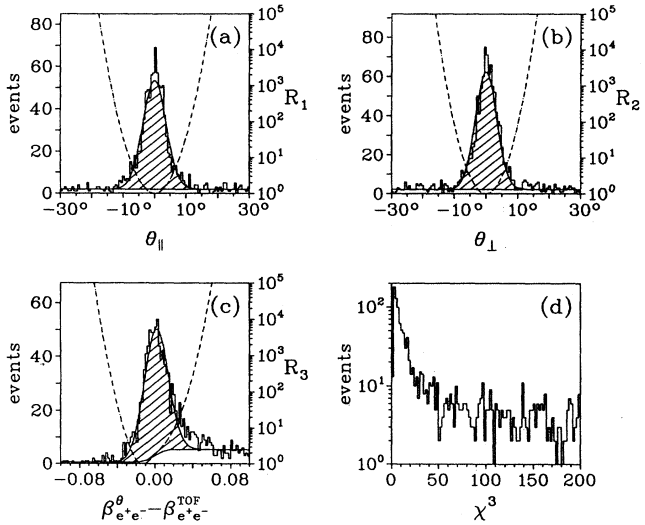

FIG. 3. Distributions of $\theta_\parallel$, $\theta_\perp$, $\beta^{\theta}_{e^+e^-} - \beta^{\rm TOF}_{e^+e^-}$, and χ^3 (see text) for events with $T_{\rm tot} > 125$ MeV and β_n outside the π^0 peak. In the first three histograms only those events were accepted which fall inside the ranges of all three histograms. The hatched areas indicate the contribution S from unperturbed three-body events as assumed in the analysis. The dashed curves are the corresponding distributions for the normalized background-to-signal ratio R.

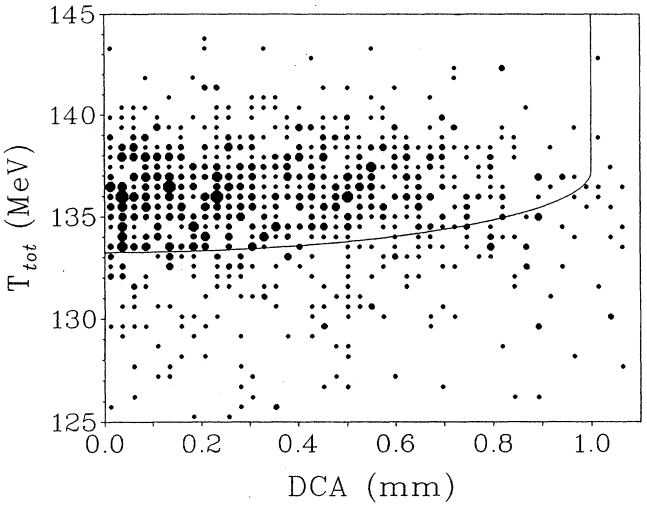

FIG. 4. Distribution of total kinetic energy $T_{\rm tot}$ vs the distance of closest approach between the two tracks (DCA) for events with $\chi^3<35$ and with a value for β_n outside the π^0 peak. The contour indicates the area accepted for three-body events.

IV. RESULTS

In Fig. 5 the β_n distributions of three different event samples are shown. For Fig. 5(a) events were selected with $T_{\rm tot}$ in the range 100–125 MeV and $\chi^3<150$, where the neutron peak from $\pi^- p\to\pi^0 n$ followed by $\pi^0\to e^+e^-X$ appears most pronounced. Figure 5(b) shows distributions of e^+e^-n events satisfying the $T_{\rm tot}$-DCA requirement for unperturbed neutrons ($\chi^3<35$) and for background neutrons ($100<\chi^3<200$). The background distribution has been normalized to the same χ^3 window. In the distribution of Fig. 5(b) the number of events at the position of the π^0 peak is slightly less than expected from the neighboring regions, so there is no indication of a contribution from π^0 decays. The 90%-confidence upper limit on $\hat{n}_\pi$, the expected number of π^0 decays, has been calculated under the assumption of a linear β_n distribution. The intercept β_0 and the expected number of background events $\hat{n}_c$ were treated as additional free parameters, giving the following probability distribution (see, for example, Ref. 21):

$$P(\hat{n}_\pi,\hat{n}_c,\beta_0)\propto\prod_{i=1}^{N}\hat{n}_i^{\,n_i}e^{-\hat{n}_i},\quad \hat{n}_i=\hat{n}_c f_i+\hat{n}_\pi g_i\ ,$$
$$f_i\propto\beta_{n,i}-\beta_0,\quad \sum_{i=1}^{N}f_i=\sum_{i=1}^{N}g_i=1\ , \tag{5}$$

where i is the channel number, N the number of channels, and n_i the measured distribution. The shape of the π^0 distribution g_i is taken from Fig. 5(a). As an example, the distribution for $n_\pi=12$, corresponding to the previous experimental value for the $\pi^0\to e^+e^-$ branching ratio, is plotted in Fig. 5(b). The probability function for $\hat{n}_\pi$, is obtained by integration over $\hat{n}_c$ and β_0:

$$\mathcal{P}(\hat{n}_\pi)=\int\int P(\hat{n}_\pi,\hat{n}_c,\beta_0)d\hat{n}_c d\beta_0\ . \tag{6}$$

The function $\mathcal{P}$, shown in Fig. 6, has been extended to unphysical negative values of $\hat{n}_\pi$. The maximum of $\mathcal{P}$ is reached for $\hat{n}_\pi=-6.2$ and the 68.3% confidence interval is $-11.3<\hat{n}_\pi<-0.3$. The distribution of the confidence level (C.L.) for $\hat{n}_\pi^{\max}$, the upper limit on $\hat{n}_\pi$, was calculated by constraining $\hat{n}_\pi$ to be positive:

$$\text{C.L.}(\hat{n}_\pi^{\max})=\int_0^{\hat{n}_\pi^{\max}}\mathcal{P}(\hat{n}_\pi)d\hat{n}_\pi\Big/\int_0^{\infty}\mathcal{P}(\hat{n}_\pi)d\hat{n}_\pi\ . \tag{7}$$

The upper limit on the number of π^0 decays at C.L. $=90\%$ is $\hat{n}_\pi^{\max}=8.0$. The corresponding upper limit on the $\pi^0\to e^+e^-$ branching ratio has been determined from the level of $\pi^- p\to e^+e^-n$ events at the π^0 peak. The fitted number of $\pi^- p\to e^+e^-n$ events in the interval $0.0297<\beta_n<0.0300$ is 11.5 ± 0.6 after correction for the background of accidental and scattered neutrons. Events

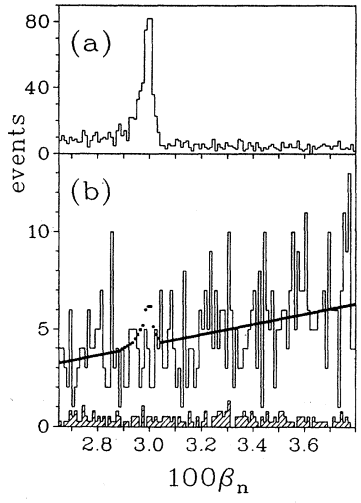

FIG. 5. Distributions of β_n for (a) π^0 decays and (b) three-body events selected by the $T_{\rm tot}$-DCA cut. The hatched area in (b) indicates the contribution of background neutrons. The dotted distribution is expected for $B_{\pi^0\to e^+e^-}=1.8\times10^{-7}$.

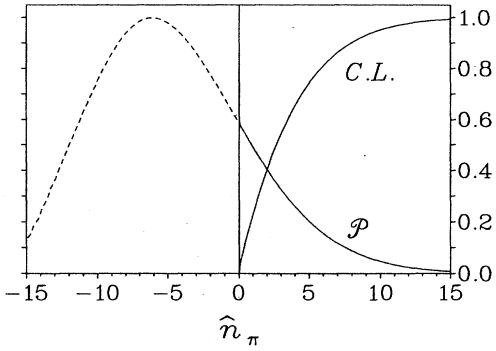

FIG. 6. Distributions of the likelihood $\mathcal{P}$ for $\hat{n}_\pi$, the expected number of π^0 decays in the three-body sample, and the confidence level (C.L.) for the upper limit on $\hat{n}_\pi$.

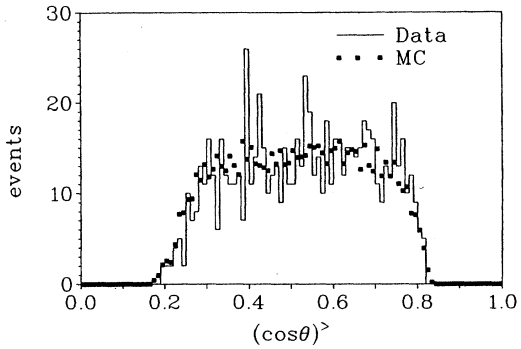

FIG. 7. Distributions of $\cos\theta$ for measured three-body events and simulated $\pi^- p \to e^+e^- n$ events, where θ is the angle between the lepton direction and the beam direction. Only the larger one of the two values of the e^+e^- pair has been incremented.

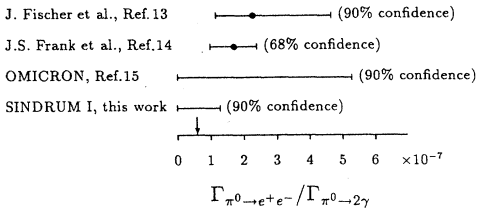

FIG. 8. Experimental values for the $\pi^0 \to e^+e^-$ branching ratio. For finite results the most likely value is indicated by a dot. The arrow points at the value for the QED prediction of about 6×10^{-8}.

of the reaction $\pi^- p \to e^+e^- n$ have been simulated using a matrix element given in Ref. 22, which is based on a treatment of the inverse reaction by Adler and Gilman[23] with corrections from Ref. 24. The resulting rate in the 3×10^{-4} interval of β_n is 1.77×10^{-7} per π^0. Radiative corrections are automatically taken into account since these are $\approx -10\%$ for both $\pi^0 \to e^+e^-$ (Ref. 25) and $\pi^- p \to e^+e^- n$ (Ref. 26). As was mentioned by Frank *et al.*,[14] this correction would raise their value for the $\pi^0 \to e^+e^-$ branching ratio by 7.4%. The measured value for the β_n intercept is $\beta_0 = (1.5\pm0.3)\%$, in agreement with the predicted value of $\beta_0 = (1.6\pm0.3)\%$. A further check of the understanding of the $\pi^- p \to e^+e^- n$ events has been made using the parametrization

$$N(\cos\theta', \beta_{e^+e^-}) \propto 1 + a(\beta_{e^+e^-})\cos^2\theta' , \tag{8}$$

where θ' is the angle between lepton and neutron in the e^+e^- c.m. system. For the two-step process $\pi^- p \to \pi^0 n$, $\pi^0 \to e^+e^-$: $a = 0$. For the reaction $\pi^- p \to e^+e^- n$ with $\beta_{e^+e^-}$ around the π^0 peak $a(\beta_{e^+e^-}) \approx 7\%$; This leads to a slightly lower acceptance. In Fig. 7 distributions of the cosine of the lepton emission angle θ relative to the beam direction are shown for measured and simulated events. Since the two $\cos\theta$ values of the e^+e^- pair are strongly correlated only $(\cos\theta)^>$, the larger one of the two has been incremented. The lowest value of $(\cos\theta)^>$ occurs for symmetric decays $(\cos\theta)^> = (\cos\theta)^< = \beta_{e^+e^-}$, whereas the maximum value is given by the hodoscope acceptance, $\cos\theta < 0.8$. The shape of the distribution is determined by $a(\beta_{e^+e^-})$, by the acceptance of the innermost wire chamber, and by the π^- stop distribution in the target. The mean e^+e^- acceptance deduced from the event simulation is $63.3\pm0.4\%$ for $\pi^- p \to e^+e^- n$ at $\beta_{e^+e^-} = \beta_{\pi^0}$ and $64.0\pm0.4\%$ for $\pi^0 \to e^+e^-$. The ratio between these two values is the only result of the Monte Carlo simulation used in the determination of the $\pi^0 \to e^+e^-$ branching ratio.

The simulation program predicts 0.5 events in the final sample which originate from the other π^0 decay modes. Since none of the processes give a dominant contribution to the total spectrum anywhere in the measured region of phase space, it is difficult to check the simulation and estimate the systematic uncertainty in this prediction. For this reason the small π^0 background has been set to zero in the determination of the upper limit on the $\pi^0 \to e^+e^-$ branching ratio. The result is

$$B_{\pi^0 \to e^+e^-} < 1.3\times10^{-7} \quad (90\% \text{ confidence level}) .$$

V. CONCLUSIONS

The result of this search for the decay $\pi^0 \to e^+e^-$ is compared with previous experiments in Fig. 8. The new upper limit gives a considerable reduction in the range of values for the branching ratio allowed by experiment and there appears to be no need to invoke the nonelectromagnetic contributions to the decay which were suggested by these earlier results. There is still a need, however, for improved experiments to detect an unambiguous signal of the decay.

This experiment is limited both by the low number of expected $\pi^0 \to e^+e^-$ events (four events at the predicted branching ratio) and by the relatively high level of $\pi^- p \to e^+e^- n$ background (15 events in a time-of-flight window corresponding to the FWHM of the resolution function). The $\pi^0 \to e^+e^-$ event rate is mainly restricted by the rate of tagged π^0's which is strongly affected by the solid angle and efficiency of the neutron detector. The background level is proportional to the neutron time-of-flight resolution. As a consequence major improvements of the method would require modifications especially in the neutron detection.

ACKNOWLEDGMENTS

We thank Bernard Coadou, René Gaubert, Albert Godin, and Jean Louis Peyrat for the design and construction of a very reliable liquid-hydrogen target and control system. Contributions from Manfred Daum, Christoph Grab, Sabine Heyer, Norbert Kraus, Dieter Renker, and Hubert Simma are gratefully acknowledged. This work was supported by the Swiss National Science Foundation and by the Natural Sciences and Engineering Research Council of Canada.

*Present address: University of Victoria, c/o TRIUMF, Vancouver, Canada V6T 2A3.
†Permanent address: Institute for Nuclear Studies, PL-05-400 Swierk, Poland.

[1]L. G. Landsberg, Phys. Rep. **128**, 301 (1985).
[2]K. S. Babu and E. Ma, Phys. Lett. **119B**, 449 (1982).
[3]A. N. Kamal and Lo Chong-Huah, Phys. Rev. D **32**, 1744 (1985).
[4]L. Bergström, Z. Phys. C **14**, 129 (1982).
[5]L. Bergström, E. Massó, Ll. Ametller, and A. Bramon, Phys. Lett. **126B**, 117 (1983).
[6]E. Massó, Phys. Lett. B **181**, 388 (1986).
[7]P. Herczeg, Phys. Rev. D **16**, 712 (1977).
[8]A. Soni, Phys. Lett. **52B**, 332 (1974).
[9]J. C. Pati and A. Salam, Phys. Rev. D **11**, 1137 (1975).
[10]J. D. Davies, J. G. Guy, and R. K. P. Zia, Nuovo Cimento **24A**, 324 (1974).
[11]H. Burkhardt, R. K. P. Zia, and J. D. Davies, J. Phys. A **7**, 40 (1974).
[12]Particle Data Group, G. P. Yost *et al.* Phys. Lett. B **204**, 1 (1988).
[13]J. Fischer, P. Extermann, O. Guisan, R. Mermod, B. Morel, L. Rosselet, R. Sachot, P. Bloch, G. Bunce, B. Devaux, A. M. Diamant-Berger, N. Do-Duc, G. Marel, and R. Turlay, Phys. Lett. **73B**, 364 (1978).
[14]J. S. Frank, C. M. Hoffman, R. E. Mischke, D. C. Moir, J. S. Sarracino, P. A. Thompson, and M. A. Schardt, Phys. Rev. D **28**, 423 (1983).
[15]A. G. Zephat, S. M. Playfer, W. van Doesburg, T. Bressani, E. Chiavassa, S. Costa, J. D. Davies, G. Dellacasa, C. W. E. van Eijk, M. Gallio, J. V. Jovanovich, G. Kernel, W. Lourens, J. Lowe, E. G. Michaelis, A. Musso, F. Sever, F. Siohan, A. Stanovik, and N. W. Tanner, J. Phys. G **13**, 1375 (1987).
[16]C. Niebuhr. Ph.D. thesis, Eidgenössische Technische Hochschule Zürich, 1989.
[17]SINDRUM Collaboration, W. H. Bertl, S. Egli, R. Eichler, R. Engfer, L. Felawka, Ch. Grab, E. A. Hermes, N. Kraus, N. Lordong, J. Martino, H. S. Pruys, A. van der Schaaf, and H. K. Walter, Nucl. Phys. **B260**, 1 (1985).
[18]L. P. Wishart *et al.*, Nucl. Instrum. Methods **57**, 237 (1967).
[19]Manufactured by Nuclear Enterprises Limited, Edinburgh, Scotland.
[20]J.-M. Weber, Master's thesis, l'Université de Luxembourg, 1985.
[21]B. Escoubes, S. de Unamuno, and O. Helene, Nucl. Instrum. Methods **A257**, 346 (1987).
[22]H. Fonvieille, Ph. D. thesis, l'Université de Clermont-Ferrand II, 1984.
[23]S. L. Adler and F. J. Gilman, Phys. Rev. **152**, 1460 (1966).
[24]G. Benfatto, F. Nicolò, and G. C. Rossi, Nuovo Cimento **14A**, 425 (1973).
[25]L. Bergström, Z. Phys. C **20**, 135 (1983).
[26]G. Bonneau and F. Martin, Nucl. Phys. **B27**, 381 (1971).